# Opposing Effects of Na$^+$ and K$^+$ on the Thermal Stability of Na$^+$,K$^+$-ATPase

Sergio B. Kaufman, F. Luis González-Flecha, and Rodolfo M. González-Lebrero*

Instituto de Química y Fisicoquímica Biológicas and Departamento de Química Biológica, Facultad de Farmacia y Bioquímica, Universidad de Buenos Aires, Buenos Aires, Argentina

Ⓢ *Supporting Information*

ABSTRACT: Folding and structural stability are key factors for the proper biological function of proteins. Na$^+$,K$^+$-ATPase is an integral membrane protein involved in the active transport of Na$^+$ and K$^+$ across the plasma membrane. In this work we characterized the effects of K$^+$ and Na$^+$ on the thermal inactivation of Na$^+$,K$^+$-ATPase, evaluating both catalytic and transport capacities of the pump. Both activities of the enzyme decrease with the preincubation time as first-order kinetics. The thermal inactivation of Na$^+$,K$^+$-ATPase is simultaneous with a conformational change detected by tryptophan and 1-aniline-8-naphtalenesulfonate (ANS) fluorescence. The kinetic coefficient of thermal inactivation was affected by the presence of Na$^+$ and K$^+$ (or Rb$^+$) and the temperature of the preincuabtion media. Our results show that K$^+$ or Rb$^+$ stabilize the enzyme, while Na$^+$ decreases the stability of Na$^+$,K$^+$-ATPase. Both effects are exerted by the specific binding of these cations to the pump. Also, we provided strong evidence that the Rb$^+$ (or K$^+$) stabilization effect is due to the occlusion of these cations into the enzyme. Here, we proposed a minimal kinetic model that explains the behavior observed in the experimental results and allows a better understanding of the results presented by other researchers. The thermal inactivation process was also analyzed according to Kramer's theory.
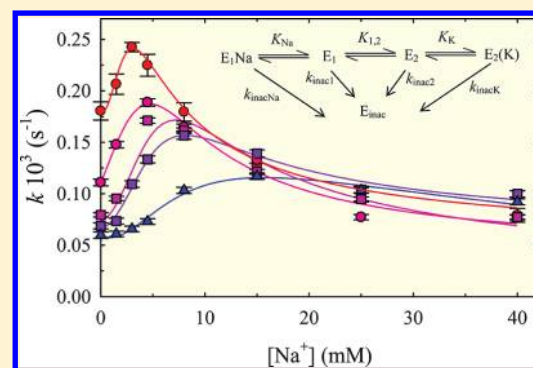
INTRODUCTION

Na$^+$,K$^+$-ATPase is an integral membrane protein involved in the active transport of Na$^+$ and K$^+$ across the plasma membrane.[1] This enzyme consists of two subunits: α (1016 residues) and β (302 residues).[2] A γ-subunit (an FXYD-protein of 64–70 residues) usually is associated with the $\alpha\beta$ oligomer. The α-subunit has a transmembrane domain formed by 10 helical segments (named M1-M10) including the cation transport sites, and three characteristic cytoplasmic domains: the actuator (A), nucleotide-binding (N), and phosphorylation (P) domains.[3–5] The β-subunit has a large extracellular portion that is glycosylated and is anchored to the membrane by a single helical segment. It is generally believed that the β-subunit has a key role in the binding/occlusion of K$^+$.[5] The γ-subunit modulates the Na$^+$,K$^+$-ATPase activity.[6] Studies on the function and crystal structures of the pump indicate that K$^+$ transport sites I and II are located within the transmembrane helices M4, M5, and M6.[4,5,7,8]

Na$^+$,K$^+$-ATPase couples ATP hydrolysis to the active transport of three Na$^+$ ions out and two K$^+$ ions into the cell.[1] The reaction cycle of the enzyme includes the following: (i) the formation and breakdown of a phosphoenzyme intermediary, (ii) conformational changes of the enzyme between the E$_1$ and E$_2$ conformers, and (iii) occlusion/deocclusion of Na$^+$ and K$^+$ ions.[9] The E$_1$ and E$_2$ conformers can be promoted by the presence of Na$^+$ and K$^+$, respectively,[10,11] and in the absence of ATP, Na$^+$, and Mg^{2+},

two K$^+$ ions are occluded in the E$_2$ conformer, E$_2$(K$_2$).[9,12–15] Biochemical and biophysical evidence support the idea that the structure of the enzyme in E$_2$(K$_2$) is rather different from that in E$_1$.[3,16–21]

Folding and structural stability are key factors for the proper biological function of proteins. It is known that forces involved in protein folding, as well as in unfolding, are closely related to the properties of the surrounding medium, which determine the stability of these structures.[22] In this way, disruption of the native three-dimensional conformations occurs as a consequence of environmental alterations such as changes in temperature, pressure, or the addition of chaotropic chemical compounds. Although thermal denaturation of soluble proteins is a well-characterized process, little is known about the stability of membrane proteins.[23] The few reports on this topic have shown that membrane proteins either undergo irreversible unfolding, regardless of whether they are folded in their natural membrane, or are solubilized, purified and reconstituted in artificial systems such as mixed micelles or bilayers.[24–29] These studies have also suggested that the transmembrane region of membrane proteins is significantly more stable than water-exposed domains.[22]

Thermal inactivation has been used as a tool to study $\alpha-\beta$ interactions and the domain structure of Na$^+$,K$^+$-ATPase.[30−34] Additionally, some studies have described the influence of natural ligands of the enzyme on its thermal inactivation.[35,36] In this work, we characterized the effects of K$^+$ and Na$^+$ on the thermal inactivation of Na$^+$,K$^+$-ATPase, by evaluating its catalytic and transport capacities and the conformation of the pump.

■ EXPERIMENTAL METHODS

Enzyme Preparation. Na$^+$/K$^+$-ATPase partially purified from pig kidney outer medulla according to the procedure of Jensen et al. was kindly provided by the Department of Biophysics, University of Århus, Denmark.[37,38] The specific activity of the preparation in optimal conditions (150 mM NaCl, 20 mM KCl, 3 mM ATP, 4 mM MgCl$_2$, and 25 mM imidazole−HCl, pH 7.4) was 24−28 μmol Pi min^{-1} (mg protein)$^{-1}$ at 37 °C.

Reagents and Reaction Conditions. [^{86}Rb]RbCl and [γ-^{32}P]ATP were obtained from Perkin-Elmer NEN Life Sciences (USA). All other reagents were of analytical grade. Measurements were performed at 25 °C and pH 7.4 in a medium containing 0.25 mM EDTA and either 25 mM imidazole−HCl (activity and occlusion measurements) or 25 mM Tris-HCl (fluorescence determinations). The concentrations of other components for each experiment are indicated in the Results section.

Determination of Na$^+$,K$^+$-ATPase Activity. Na$^+$,K$^+$-ATPase activity was determined according to Schwarzbaum et al.,[39] by measuring the amount of [^{32}P]Pi released from [γ-^{32}P]ATP. In all cases, the incubation times were short to avoid the hydrolysis of more than 10% of ATP during the assay and to ensure initial rate conditions. The reactions were carried out at 25 °C in a medium containing 150 mM NaCl, 20 mM KCl, 3 mM [γ-^{32}P]ATP, and 4 mM MgCl$_2$.

Rb$^+$ Occlusion in Equilibrium Conditions. Na$^+$/K$^+$-ATPase was incubated for 15 min in a medium containing [^{86}Rb]RbCl at 25 °C. Then, the amount of occluded Rb$^+$ (Rb$_{occ}$) was measured following the procedure described by Rossi et al.[40] The blank values, estimated from the amount of ^{86}Rb$^+$ retained by the filters in the absence of enzyme, were usually much lower than 10% of the amount of occluded ^{86}Rb$^+$.

Fluorescence Measurements. Steady state fluorescence measurements were performed using a SLM-Aminco Bowman series 2 spectrofluorometer at 25 °C in a 3 × 3 mm quartz cuvette. Emission spectra of Na$^+$,K$^+$-ATPase were recorded between 305 and 400 nm after excitation at 295 nm. Both excitation and emission bandwidths were set at 4 nm. The spectra were corrected for background emission (without enzyme). We used 25 mM Tris-ClH instead of imidazole−ClH because the latter shows fluorescence in the same spectral region as tryptophan. 1-Aniline-8-naphtalenesulfonate (ANS) fluorescence was recorded between 420 and 550 nm following excitation at 380 nm (bandwidths were set at 8 nm). Total intensity (I_t) was calculated as the sum of the fluorescence intensities recorded.

Circular Dichroism Measurements. Circular dichroism spectra of Na$^+$,K$^+$-ATPase were recorded at 298 K in the wavelength region of 200−250 nm using a Jasco J-810 spectropolarimeter, as described previously.[41] Data were collected in a 1 mm path length cuvette using a scan speed of 20 nm/min with a time constant of 1 s.

Inactivation Protocol. A volume of 100 μL of enzyme suspension (0.15−0.5 mg of protein/mL) at room temperature was mixed with 400 μL of a solution at the temperature used in each experiment (49−57 °C) and then incubated for different periods of time (4−170 min). The time to reach the inactivation temperature was, in all cases, not longer than 15 s. After incubation, the reaction tubes were placed in an ice−water bath to rapidly drop the temperature and stop the inactivation reaction and then left for 3−5 min. The tubes were then placed in a 25 °C bath for 10 min prior to the determinations.

Data Analysis. Equations were adjusted to the experimental data by nonlinear regression. The best fitting values of the parameters are expressed as mean ± standard error.

■ RESULTS

Thermal Inactivation in the Absence of Ligands. Thermal inactivation of Na$^+$,K$^+$-ATPase was studied by incubating the enzyme preparation (hereinafter: preincubation) for different time periods at several temperatures. Then Na$^+$,K$^+$-ATPase activity and the amount of occluded Rb$^+$ (Rb$_{occ}$) were measured. It is important to point out that Rb$^+$ occlusion was carried out through the so-called *direct route of occlusion*, i.e. in a medium without Na$^+$, Mg^{2+}, and ATP, where the enzyme is in equilibrium distribution between free and occluded Rb$^+$.

Figure 1A shows the variation in Na$^+$,K$^+$-ATPase activity and Rb$_{occ}$ as a function of the preincubation time at 52 °C in the absence of ligands. It can be seen that both Na$^+$,K$^+$-ATPase activity and Rb$_{occ}$ decreased following a single exponential decay function of the preincubation time.

$$M_t = M_0 e^{-kt} \tag{1}$$

where M_t and M_0 are either the Na$^+$,K$^+$-ATPase activity or Rb$_{occ}$ at each preincubation time (t) or $t = 0$, respectively, and k is the thermal inactivation rate coefficient. The best fitting values of k for Na$^+$,K$^+$-ATPase activity and Rb$_{occ}$ were not significantly different, thus suggesting that both measurements are the expression of the same phenomenon.

Similar thermal inactivation experiments were performed at various temperatures in the range between 49 and 57 °C, and the thermal inactivation rate coefficients (k) were obtained (Figure 1B). The variation in k with the preincubation temperature can be described by

$$k = A e^{-E_a/RT} \tag{2}$$

where A is the pre-exponential factor, E_a, the activation energy, R, the gas constant, and T, the absolute temperature.

To test whether the decay of Rb$_{occ}$ occurs by a decrease in the capacity and/or in the affinity of the enzyme to occlude Rb$^+$, we measured the amount of occluded Rb$^+$ as a function of the concentration of this cation, using a fully active and partially inactivated enzyme preparation (Figure 2). In both cases, Rb$_{occ}$ showed a hyperbolic behavior with the Rb$^+$ concentration and can be described by

$$Rb_{occ} = \frac{Rb_{occ,\infty}[Rb^+]}{[Rb^+] + K_{0.5}} \tag{3}$$

The maximal amount of occluded Rb$^+$ (Rb$_{occ,\infty}$) was 5.43 ± 0.13 nmol Rb$^+$ (mg prot)$^{-1}$ for the native enzyme and 1.66 ± 0.03 nmol Rb$^+$ (mg prot)$^{-1}$ for the partially inactivated enzyme. On the other hand, the apparent affinity of the enzyme for Rb$^+$
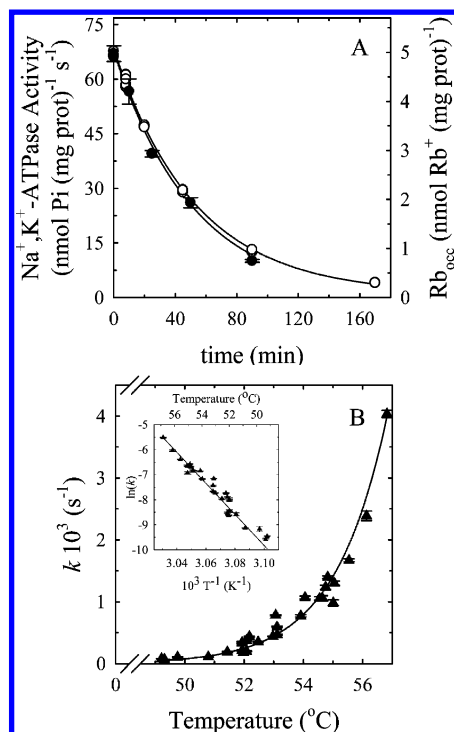
3422

dx.doi.org/10.1021/jp2124108 | J. Phys. Chem. B 2012, 116, 3421−3429

Figure 1. Na$^+$,K$^+$-ATPase thermal inactivation in the absence of ligands. Panel A shows the remained Na$^+$,K$^+$-ATPase activity (●) and the amount of occluded Rb$^+$ (○) plotted as a function of the preincubation time. The continuous lines in panel A are plots of eq 1 for k and M_0, respectively, equal to $(0.325 \pm 0.017) \times 10^{-3}$ s^{-1} and 67.72 ± 0.97 nmol Pi (mg prot)$^{-1}$ s^{-1} for Na$^+$,K$^+$-ATPase and $(0.315 \pm 0.012) \times 10^{-3}$ s^{-1} and 5.000 ± 0.066 nmol Rb$^+$ (mg prot)$^{-1}$ for Rb$_{occ}$. Panel B shows the best fitting values of k plotted as a function of the preincubation temperature. The inset shows the corresponding Arrhenius plot. The continuous line is the plot of eq 2 with the best fitting parameter values ($\ln(A) = 181.9 \pm 9.6$ and $E_a = 122.8 \pm 6.2$ kcal mol^{-1}).
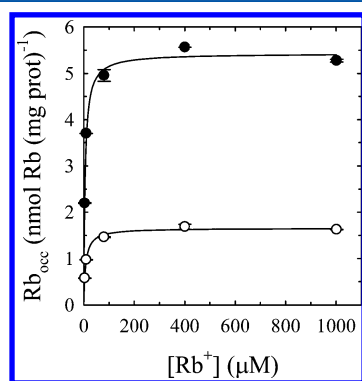

Figure 2. Equilibrium distribution between free and occluded Rb$^+$ for fully and partially inactivated enzyme. Rb$_{occ}$ was measured on a partially inactivated enzyme preparation (30% remaining ATPase activity) obtained by preincubation for 60 min at 52 °C (○) and a noninactivated control (●). The continuous lines are the plot of eq 3 fitted to the experimental data.

($K_{0.5}$) did not vary significantly (5.34 ± 0.68 and 7.39 ± 0.74 μM for the fully and partially activated enzyme, respectively). This result indicates that the loss in Rb$^+$ occlusion is due mainly to an inactivation of the enzyme and not to a change in its Rb$^+$ affinity.

Structural Changes Associated with Thermal Inactivation in the Absence of Ligands. The effect of the preincubation at high temperatures on the secondary and tertiary structure of the enzyme was explored by recording far UV circular dichroism (CD), tryptophan fluorescence spectra, and ANS fluorescence.

Na$^+$,K$^+$-ATPase is a helical membrane protein that contains 11 tryptophan residues situated in the membrane region, 2 in the ATP-binding region, and 1 in the extracellular region of the β-subunit.[4,5] Additionally, Trp quenching experiments with a lipidic acceptor[42] and Trp lifetime distribution analysis[43] have indicated that Trp fluorescence is predominantly due to the residues located in the membrane region.

The far UV CD spectra of the active and thermally inactivated protein showed slight but not significant differences (Figure 3A), indicating that the secondary structure of the enzyme was not mainly affected by the thermal inactivation treatment. Additionally, both spectra showed characteristic features of alpha helical proteins.

Figure 3B shows the tryptophan fluorescence spectra of Na$^+$,K$^+$-ATPase preincubated for different periods of time at 54.3 °C. The spectrum of the native enzyme excited at 295 nm is centered on 340 nm, which is characteristic of Trp in hydrophobic environments. Total Trp fluorescence intensity (I_{Trp}) decreased along a single exponential function of preincubation time plus a time-independent term. Additionally, a slight blue shift of the center of the spectral mass (about 4 nm) was observed upon enzyme inactivation, thus suggesting that Trp residues exposed to the aqueous environment are the most affected.

The size of hydrophobic patches of proteins are usually explored using the fluorescence probe ANS.[44] Na$^+$,K$^+$-ATPase was preincubated for different periods of time at 54.3 °C, and after addition of ANS, the fluorescence spectra of the probe were recorded (inset in Figure 3C). The total ANS fluorescence intensity (I_{ANS}) increased with the preincubation time along a single exponential function (Figure 3C). The increase in I_{ANS} indicates that thermal inactivation causes a relaxation of the enzyme structure, which exposes hydrophobic cavities that were hidden in the native structure.

The best fitting values of the inactivation rate coefficient (k) obtained from I_{Trp} ($(0.369 \pm 0.033) \times 10^{-3}$ s^{-1}) and I_{ANS} ($(0.45 \pm 0.17) \times 10^{-3}$ s^{-1}) measurements were not significantly different to that obtained measuring the enzyme activity ($(0.388 \pm 0.010) \times 10^{-3}$ s^{-1}) in the presence of Tris-HCl instead of imidazole−HCl. This correlation was also verified at several temperatures (Supporting Information Figure S1). This suggests that the enzyme inactivation is associated with structural changes in the protein. However, these changes seemed to be small since no differences were detected in the secondary structure.

Effect of K$^+$ and Rb$^+$ on Thermal Inactivation. Thermal inactivation of Na$^+$,K$^+$-ATPase was studied in the presence of K$^+$ or Rb$^+$. At a given temperature, the inactivation rate coefficients (k) decreased with the increase in cation concentration, up to a small constant value (Figure 4A).

$$k = \frac{(k_0 - k_\infty)K_{0.5}}{K_{0.5} + [X^+]} + k_\infty \quad (4)$$

where $[X^+]$ represents the concentration of K$^+$ or Rb$^+$. The $K_{0.5}$ values increased from 0.138 ± 0.021 to 3.64 ± 0.74 mM, when
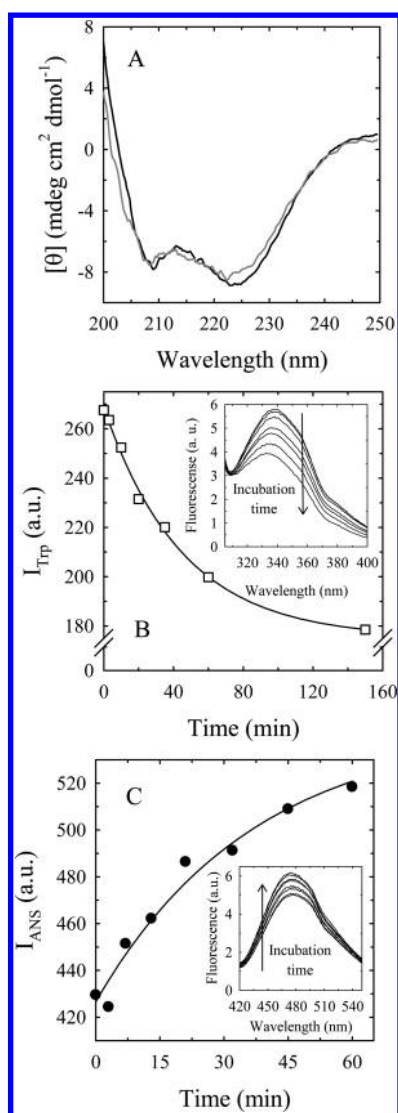
Figure 3. Structural changes and enzyme inactivation. Panel A shows the far UV CD spectra of native (black line) and inactivated enzyme (gray line, 150 min at 54.3 °C). Each spectrum is the average of three consecutive spectra of the same sample. The Na$^+$,K$^+$-ATPase or ANS fluorescence spectrum was recorded at 25 °C after various preincubation times at 54.3 °C (insets in B and C, respectively). Tris-HCl was used as a buffer instead of imidazole–HCl From each of these spectra, we calculated the total fluorescence intensity for Na$^+$,K$^+$-ATPase and ANS (I_{Trp} or I_{ANS}, respectively) and plotted it as a function of the preincubation time (B and C). The continuous lines in B and C are the best fitting plots of eq 1 plus a time-independent constant.

the preincubation temperature varied from 55 to 58 °C (inset in Figure 4A).

Na$^+$,K$^+$-ATPase activity was measured as a function of the preincubation time at different temperatures in the presence of 40 mM K$^+$ or Rb$^+$ to ensure maximal effects of these cations. The best fitting values of the thermal inactivation rate coefficient (k) are shown in Figure 4B. The values of k increased exponentially with the preincubation temperature according to a linear Arrhenius plot (inset in Figure 4B) with activation energy (E_a) values of 159 ± 11 (Rb$^+$) and 151 ± 15 kcal mol^{-1} K^{-1} (K$^+$).

It has been previously proposed that Rb$^+$ protects Na$^+$,K$^+$-ATPase against thermal inactivation by its occlusion in the
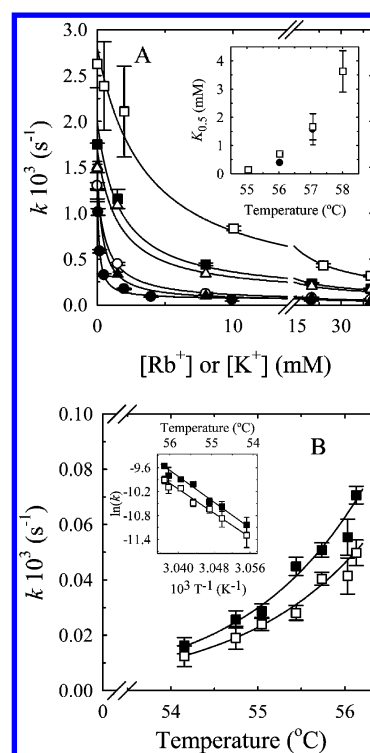

Figure 4. Effect of K$^+$ and Rb$^+$ on thermal inactivation of Na$^+$,K$^+$-ATPase. Panel A shows the dependence of the thermal inactivation rate coefficient (k in eq 1) either on [Rb$^+$] at 55 (●), 56 (○), 57 (■), and 58 (□) °C or on [K$^+$] at 56 (△) and 57 (▲) °C. The continuous lines are plots of eq 4 for the best fitting values of k_0, k_∞, and $K_{0.5}$ obtained at each preincubation temperature. The best fitting values of $K_{0.5}$ in the presence of Rb$^+$ (□) or K$^+$ (●) are plotted as a function of temperature in the inset in panel A. The values of k shown in panel B were obtained by fitting eq 1 to inactivation experiments at different preincubation temperatures in the presence of 40 mM of either Rb$^+$ (■) or K$^+$ (□). An Arrhenius plot of these data is shown in the inset in panel B. The continuous lines in panel B are plots of eq 2 for ln(A) and E_a, respectively, equal to 233 ± 17 and 159 ± 11 kcal mol^{-1} for Rb$^+$ and 221 ± 22 and 151 ± 15 kcal mol^{-1} for K$^+$.

protein.[36] However, this effect of Rb$^+$ could also be explained as a consequence of its binding to the cytoplasmic nontransport K$^+$/Rb$^+$ site in the P-domain of the enzyme.[45–47] These hypotheses were tested by measuring Rb$_{occ}$ as a function of the preincubation time at 55 °C and several Rb$^+$ concentrations (Figure 5A). By fitting eq 1 to these data, we obtained the values of Rb$_{occ}$ at $t = 0$ (Rb$_{occ,0}$) and k for each Rb$^+$ concentration. Rb$_{occ,0}$ and k varied hyperbolically with Rb$^+$ concentration (Figure 5B and C), $K_{0.5}$ = 0.132 ± 0.023 and 0.154 ± 0.055 mM, respectively. These values were not significantly different from each other, thus suggesting that the protection against thermal inactivation exerted by Rb$^+$ (or K$^+$) is due to the occlusion of the cations in the transport sites of the enzyme. Then, the $K_{0.5}$ values obtained in Figure 4A probably correspond to the Rb$^+$ occlusion affinity of the enzyme.

Effect of Na$^+$ on Thermal Inactivation. The effect of Na$^+$ on the thermal inactivation of Na$^+$,K$^+$-ATPase was studied including different concentrations of Na$^+$ in the preincubation medium. The thermal inactivation rate coefficients (k) showed a biphasic dependence on Na$^+$ concentration (Figure 6A). The increase in k at the lowest concentrations of Na$^+$ indicates the kinetic destabilization of the enzyme. Conversely, a stabilization
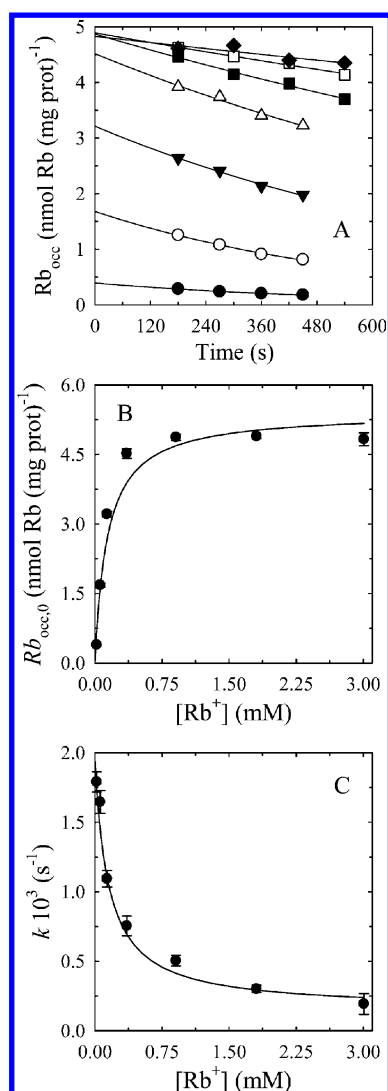
Figure 5. Thermal inactivation of Na$^+$,K$^+$-ATPase followed by Rb$^+$ occlusion. Panel A shows the amount of occluded Rb$^+$ (Rb$_{occ}$) in equilibrium conditions measured at 55 °C after preincubating the enzyme along different periods of time at 0.020 (●), 0.059 (○), 0.136 (▼), 0.356 (△), 0.907 (■), 1.807 (□), and 3.007 (◆) mM Rb$^+$. The continuous lines are plots of eq 1 for the best fitting values of M_0 (amount of occluded Rb$^+$ at time = 0, Rb$_{occ,0}$) and k. These values are plotted as a function of [Rb$^+$] in panels B and C, respectively. The continuous lines in panels B and C are plots of eqs 3 and 4 respectively with Rb$_{occ,\infty}$ = 5.27 ± 0.24 nmol Rb (mg prot)$^{-1}$, k_0 = (1.95 ± 0.17) × 10^{-3} s^{-1}, k_∞ = (0.151 ± 0.081) × 10^{-3} s^{-1}, and the values of $K_{0.5}$ given in the main text.
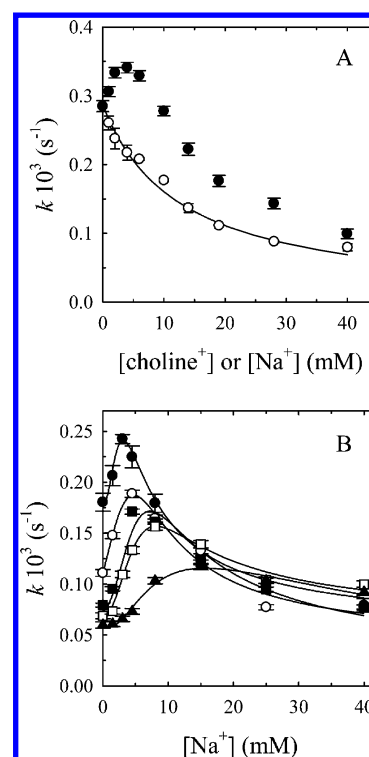

Figure 6. Effects of Na$^+$ and ionic strength on thermal inactivation of Na$^+$,K$^+$-ATPase. Panel A shows the dependence of the thermal inactivation rate coefficient (k in eq 1) on either cholineCl (○) or NaCl (●) at 52.2 °C. When cholineCl was present in the preincubation medium, the Na$^+$,K$^+$-ATPase activity measurements were carried out in the presence of 20 mM cholineCl. The continuous line in panel A is the plot of eq 4 with the best fitting parameter values: k_0 = (0.286 ± 0.004) × 10^{-3} s^{-1}, k_∞ = (0.002 ± 0.0001) × 10^{-3} s^{-1}, and $K_{0.5}$ = 12.7 ± 2.9 mM. Panel B shows the dependence of k on [NaCl] in the presence of 0 (●), 0.05 (○), 0.1 (■), 0.2 (□), and 0.5 (▲) mM RbCl. The continuous lines in panel B are plots of an empirical function to facilitate the visualization of each curve.

of the protein was observed at higher concentrations of Na$^+$. This last effect could be due to the increase in ionic strength with Na$^+$ concentration.[36] To test this, thermal inactivation experiments were carried out by replacing Na$^+$ with choline$^+$ (Figure 6A), a cation which does not specifically interact with the enzyme. A progressive stabilization of the enzyme was observed at increasing choline$^+$ concentrations, suggesting that the stabilization observed at the highest Na$^+$ concentrations is a nonspecific effect.

To test whether destabilization at low [Na$^+$] is due to the cation binding to the transport sites, and knowing that K$^+$ and Na$^+$ bind at the same sites of the enzyme,[10,11,48] we explored the dependence of k in competition experiments between Na$^+$

and K$^+$ (Figure 6B). It can be seen that at constant [K$^+$], k values show a biphasic dependence on Na$^+$ concentration, which was progressively shifted to the right as [K$^+$] increased. However, k values converged at the highest Na$^+$ concentrations, thus reinforcing the idea that the effect at high Na$^+$ concentrations is due to a nonspecific effect of ionic strength. Then, we posit that the specific effect of Na$^+$ is the destabilization of the enzyme.

The effect of Na$^+$ on thermal inactivation of the enzyme was studied at different temperatures (Figure 7). To analyze the specific effect of Na$^+$, the contribution of the ionic strength was subtracted from each curve, obtaining the Na$^+$ specific inactivation rate coefficient (k_{Na}). This contribution was quantified by fitting eq 4 to the values of k at [Na$^+$] higher than 6 mM (continuous line in Figure 7A). At each temperature, k_{Na} followed a rectangular hyperbola of [Na$^+$] plus a constant term (Figure 7B),

$$k_{Na} = \frac{(k_{Na,\infty} - k_{Na,0})[Na^+]}{[Na^+] + K_{0.5,Na}} + k_{Na,0} \qquad (5)$$

where $k_{Na,0}$ and $k_{Na,\infty}$ are the values of k_{Na} when [Na$^+$] tends to zero or infinity, respectively, and $K_{0.5,Na}$ is the Na$^+$ concentration at which the value of k_{Na} equals the average between $k_{Na,0}$ and $k_{Na,\infty}$. The best fitting values of $K_{0.5,Na}$
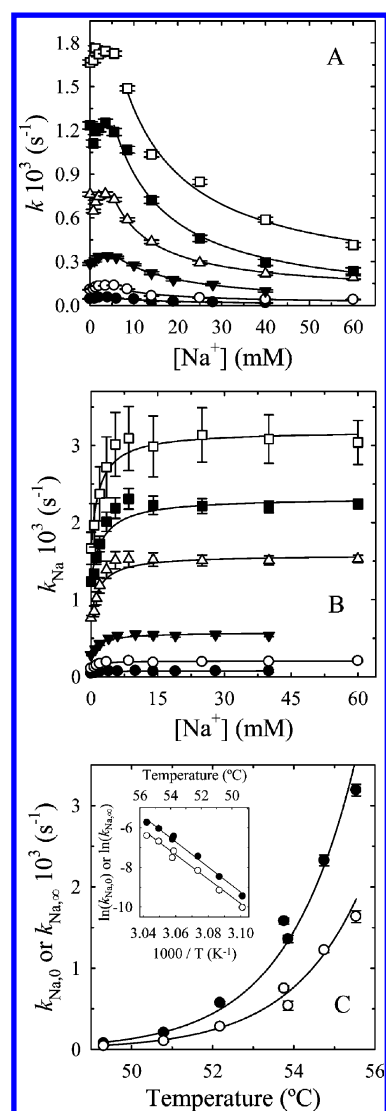
Figure 7. Na$^+$ effects on thermal inactivation of Na$^+$,K$^+$-ATPase. The k values shown in panel A were obtained at different [Na$^+$] by fitting eq 1 to inactivation experiments at 49.3 (●), 50.8 (○), 52. (▼), 53.8 (△), 54.7 (■), and 55.3 °C (□). The continuous line in A is the plot of eq 4 fitted to the values of k obtained at [Na$^+$] higher than 6 mM. Panel B shows the values of k corresponding to the Na$^+$ effect calculated as described in the main text (k_{Na}). The continuous lines are plots of eq 5 for the best fitting values of the parameters. The k_{Na} values when the Na$^+$ concentration tends to zero ($k_{Na,0}$, ○) or infinity ($k_{Na,\infty}$, ●) are plotted as a function of preincubation temperature in panel C. An Arrhenius plot of these data is shown in the inset in panel C. The continuous lines correspond to the best fitting plot of eq 2, with E_a given in the main text.

increased slightly with temperature from 1.4 ± 0.6 at 49.3 °C to 2.0 ± 0.5 mM at 55.5 °C, in contrast with the high increase observed for K$^+$ (Supporting Information Figure S2). Remarkably, the dependence of $k_{Na,0}$ and $k_{Na,\infty}$ on the temperature followed the Arrhenius law (Figure 7C). The E_a values were 122.4 ± 5.4 kcal mol^{-1} K^{-1} ([Na$^+$] = 0) and 125.7 ± 5.4 kcal mol^{-1} K^{-1} ([Na$^+$] → ∞).

■ DISCUSSION

Structure–Activity Correlations. The present study shows that the preincubation of the enzyme causes a decrease in both Na$^+$,K$^+$-ATPase activity and Rb$^+$ occlusion, with a

Scheme 1. Rb$^+$ Deocclusion and Dissociation from Na$^+$,K$^+$-ATPase

$$E_2(Rb) \xleftarrow{\quad K_{deocc} \quad} E_1Rb \xleftarrow{\quad K_{diss} \quad} E_1 + Rb^+$$

Scheme 2. Conformational Equilibria and Thermal Inactivation of Na$^+$,K$^+$-ATPase
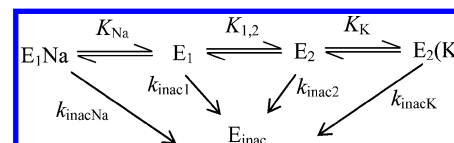
Table 1. Values for Rate and Equilibrium Constants (Scheme 2) Used for Simulations in Figure 8

$k_{inac,Na}$	2.33×10^{-3} s^{-1}	interpolated from $k_{Na,\infty}$ data in Figure 7C at 55 °C
$k_{inac,K}$	0.019×10^{-3} s^{-1}	interpolated from k_{∞} data in Figure 4A at 55 °C
$k_{inac,1}$	2.33×10^{-3} s^{-1}	assumed equal to $k_{inac,Na}$ given that Na$^+$ shifts the equilibrium toward the E$_1$ form
$k_{inac,2}$	0.019×10^{-3} s^{-1}	assumed equal to $k_{inac,K}$ given that K$^+$ shifts the equilibrium toward the E$_2$ form
$k_{inac,I}$	0.019×10^{-3} s^{-1}	assumed equal to $k_{inac,K}$[36]
$K_{1,2}$	1.52	calculated as $(k - k_{inac2})/(k_{inac1} - k)$ using the value of k interpolated from Figure 1B at 55 °C
K_{Na}	1.15 mM	calculated as $K_{0.5}K_{1,2}/(1 + K_{1,2})$ using the value of $K_{0.5}$ interpolated from Supporting Information Figure S2 at 55 °C
K_K	0.0582 mM	calculated as $K_{0.5}/(1 + K_{1,2})$ using the value of $K_{0.5}$ from data in Figure 5
K_I	12.7 mM	assumed equal to $K_{0.5}$ from the choline data in Figure 6A

simultaneous conformational change detected by intrinsic fluorescence and ANS fluorescence (Figures 1−3). In all experimental conditions and temperatures tested, we observed that these measurements varied along a single exponential function of the preincubation time (eq 1). Although this simple behavior contrasts with the large size of the enzyme and its complex structural organization, it appears to be common in P-ATPases.[28−30,35,36]

Changes in Trp and ANS fluorescence spectra suggested a partial disorganization of the enzyme structure with an increase in the exposure of the hydrophobic patches. Additionally, circular dichroism (CD) measurements showed a slight but not significant change in the secondary structure (Figure 3A). Using a better resolution CD device based on synchrotron radiation, Miles et al.[49] recently found that this small change is significant. These observations led us to believe that the structural changes caused by the preincubation result in a molten globule-like structure. Since the structural changes observed are simultaneous with the loss of Na$^+$,K$^+$-ATPase activity at all the temperatures tested (Supporting Information Figure S1), these small conformational changes would be enough to inactivate the enzyme.

Although the blue shift observed in the Trp fluorescence spectra indicates that the water-exposed regions of the enzyme are the most affected by the preincubation treatment, reduction of the Rb$^+$ occlusion capacity of the enzyme suggests that the transmembrane domain was also affected (see also ref 34). Nevertheless, we can not discard that the structural change in the nonmembrane domains or in the β-subunit can modify the
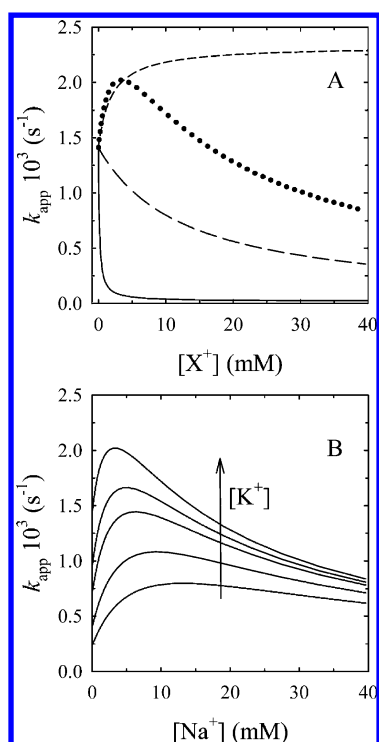
Figure 8. Simulation of the model for thermal inactivation of Na^+,K^+-ATPase. Panel A shows the values of k_{app} simulated as a function of $[K^+]$ (continuous line), cholineCl (long-dashed line), and $[Na^+]$ (dotted line). The specific effect of Na^+ was simulated without considering the effect of ionic strength (short-dashed line). Panel B shows the values of k_{app} simulated for the competition between Na^+ and the following K^+ concentrations: 0, 0.05, 0.1, 0.25, and 0.5 mM.
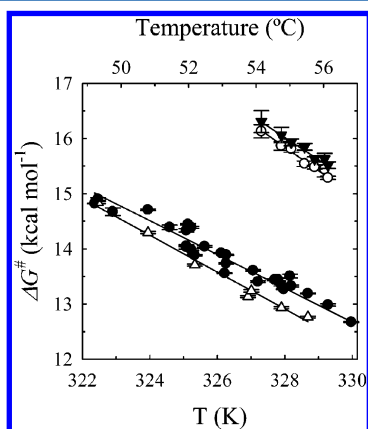

Figure 9. Free activation energy ($\Delta G^{\ddagger}$) for the different preincubation media. The values of $\Delta G^{\ddagger}$ were obtained by fitting $M_t = M_0 \exp[-\nu \eta_0/\eta_T \exp(-\Delta G^{\ddagger}/(RT))t]$ (from eq 9 into 1) to inactivation experiments in the absence of ligands (●) or in the presence of either 20 mM Rb^+ (▼) or 20 mM K^+ (○) or at $[Na^+]$ tending to infinity (△). The continuous lines are plots of $\Delta G^{\ddagger} = \Delta H^{\ddagger} - T\Delta S^{\ddagger}$ with the best fitting values shown in Table 2.

accessibility of the occlusion sites, resulting in the loss of Rb^+ occlusion without affecting the transmembrane structure.

K^+ and Rb^+ Protection. In agreement with previous reports,[30,36] we observed that the presence of K^+ (or Rb^+) during thermal inactivation caused a strong decrease in the inactivation rate (Figure 4). Additionally, our results confirm the hypothesis that Rb^+ protection is produced by the

formation of the enzyme states containing occluded Rb^+ (Figure 5A and B).

We observed a strong dependence of the Rb^+ occlusion affinity on the preincubation temperature (inset in Figure 4A), i.e. $K_{0.5}$ values for Rb^+ increased nearly 25-fold (from 0.14 to 3.64 mM) in a 3 °C interval (55−58 °C). In contrast, the $K_{0.5,Na}$ values increased slightly in a temperature range between 49 and 55 °C (Supporting Information Figure S2). This difference could be due to the fact that in our experimental conditions the Rb^+ was occluded by the enzyme while Na^+ was not.

In this sense, it is well-known that Rb^+ (or K^+) occlusion includes two steps: the cation binding and a subsequent conformational change of the protein (Scheme 1), where $E_2(Rb)$ represents the enzyme with occluded Rb^+. Then, Rb_{occ} will vary with $[Rb^+]$ as follows:

$$Rb_{occ} = \frac{\dfrac{E_T}{1 + K_{deocc}}[Rb^+]}{[Rb^+] + \dfrac{K_{diss}K_{deocc}}{1 + K_{deocc}}} \qquad (6)$$

Notice that $E_T/(1 + K_{deocc})$ and $K_{diss}K_{deocc}/(1 + K_{deocc})$ correspond to $Rb_{occ,\infty}$ and $K_{0.5}$ in eq 3, respectively.

The large increase in $K_{0.5}$ with temperature could be due to an increase in the equilibrium constant of the dissociation of Rb^+ (K_{diss}) and/or the cation occlusion (K_{deocc}). Considering that K_{diss} did not vary significantly within the temperature interval studied, as observed for Na^+ (Supporting Information Figure S2), the change in $K_{0.5}$ could be attributed to a strong temperature dependence on the enzyme conformational change that leads to Rb^+ occlusion.

Since $Rb_{occ,\infty}$ is close to twice the total amount of the enzyme (see legend to Figure 5), K_{deocc} must be much smaller than 1. Assuming that $K_{deocc} = 0.01$ at 55 °C, K_{diss} would be 14.14 mM, according to eq 6 and Figure 5.

Model of the Effects of Na^+ and K^+. In this work, we demonstrated that K^+ increased protein stability against thermal inactivation while the specific effect of Na^+ is the destabilization of the enzyme. Additionally, competition experiments between Na^+ and K^+ indicated that these effects are exerted by the specific binding of these cations to the enzyme. The equilibrium distribution between the E_1 and E_2 conformers of Na^+,K^+-ATPase could be shifted toward E_1 by the binding of Na^+ and conversely toward E_2 by K^+ binding.[10]

A minimal scheme that takes into account the conformational changes, the binding of Na^+ or K^+, and the thermal inactivation of each form is presented in Scheme 2. For the sake of simplicity, we assume that each enzyme binds only one Na^+ or K^+.

Note that the inactivation reactions that lead to the inactive enzyme (E_{inac}) are considered irreversible. Considering that the binding of the cations and the conformational change ($E_1 \Leftrightarrow E_2$) are in rapid equilibrium, with respect to the inactivation steps, the concentration of active enzyme will decrease with the preincubation time (t) according to

$$[E]_t = [E]_0 e^{-k_{app}t} \qquad (7)$$

Table 2. Thermodynamic Activation Parameters at 55 °C

	no ligands	Rb$^+$	K$^+$	Na$^+$
$k \times 10^3$ (s^{-1})	1.23 ± 0.03	0.026 ± 0.003	0.019 ± 0.004	2.33 ± 0.07
$\Delta G^{\ddagger}$ (kcal mol^{-1})	13.31 ± 0.02	15.89 ± 0.08	16.06 ± 0.13	12.93 ± 0.02
$\Delta H^{\ddagger}$ (kcal mol^{-1})	113.7 ± 7.0	157.0 ± 9.2	147 ± 15	122.4 ± 6.1
$T\Delta S^{\ddagger}$ (kcal mol^{-1})	100.4 ± 7.1	141.1 ± 9.2	131 ± 15	109.5 ± 6.1
$\Delta\Delta G^{\ddagger}$ (kcal mol^{-1})	0	2.58	2.75	−0.38
$\Delta\Delta H^{\ddagger}$ (kcal mol^{-1})	0	43.3	33.3	8.3
$\Delta(T\Delta S^{\ddagger})$ (kcal mol^{-1})	0	40.7	30.7	9.1

where $[E]_0$ and $[E]_t$ are the concentrations of the active enzyme at time 0 and t and the apparent rate constant of thermal inactivation (k_{app}) is given by

$$k_{app} = \{[K^+]K_{Na}k_{inacK} + K_K K_{Na}(K_{1,2}k_{inac1} + k_{inac2})$$
$$+ K_K K_{1,2}k_{inacNa}[Na^+]\}$$
$$/\{[K^+]K_{Na} + K_K K_{Na}(1 + K_{1,2}) + K_{1,2}K_K[Na^+]\}$$
(8)

Equation 7 is a single exponential function of time identical to eq 1, which describes the results presented both in this work and others.[28−30,35,36]

In the absence of cations, k_{app} will be equal to $(K_{1,2}k_{inac1} + k_{inac2})/(1 + K_{1,2})$. If the equilibrium is shifted toward E_1 ($K_{1,2} \to \infty$), k_{app} will tend to k_{inac1} and, conversely, if E_2 is the predominant form of the enzyme ($K_{1,2} \to 0$), k_{app} will tend to k_{inac2}. In the presence of K$^+$ or Na$^+$, k_{app} will vary with the concentration of each cation along an increasing or decreasing hyperbola from $(K_{1,2}k_{inac1} + k_{inac2})/(1 + K_{1,2})$ to k_{inacK} or k_{inacNa}. The $K_{0.5}$ of these hyperbolas will be $K_K(1 + K_{1,2})$ for K$^+$ and $K_{Na}(1 + K_{1,2})/K_{1,2}$ for Na$^+$.

The effect of ionic strength (I) can be included in Scheme 2 considering that I causes a stabilization of all the forms of the enzyme with the same half-maximum effect constant (K_I) and inactivation rate ($k_{inac,I}$).

On this basis, we simulated the variation of k_{app} as a function of [K$^+$], [Na$^+$], and [choline$^+$] at 55 °C using the values of the model constants given in Table 1. The simulated curves in Figure 8 reproduced the behavior observed in the experimental data presented in this work, thus validating the proposed model. In addition, this minimal model allows a better understanding of the results presented by Fischer, who showed that both Na$^+$ and K$^+$ stabilize the enzyme against thermal inactivation.[35] The high [Na$^+$] used by this author (100 mM) caused the stabilization of the enzyme due to the increase in ionic strength that masked the Na$^+$ destabilization demonstrated in the present work. Furthermore, considering a high value of $K_{1,2}$, the proposed model reproduced the experimental results reported by Fodor et al.[36] In these simulation conditions, all the enzyme units are in the E_1 conformation, and therefore, the destabilization effects exerted by Na$^+$ can not be observed.

Thus, the minimal model presented here is a very good approximation to the understanding of the effects of Na$^+$ and K$^+$ upon the thermal inactivation of Na$^+$,K$^+$-ATPase.

Transition State Analysis. The variation in the rate of reaction (k) with the temperature in a viscous solvent can be described by a Kramers type model,[50−55] as follows:

$$k = \nu\frac{\eta_0}{\eta_T}e^{-\Delta G^{\ddagger}/RT} = \nu\frac{\eta_0}{\eta_T}e^{-\Delta H^{\ddagger}/RT}e^{\Delta S^{\ddagger}/R}$$
(9)

where ν is the k value at the reference temperature for a barrierless process, η is the medium viscosity at the reference temperature (η_0) and at the preincubation temperature (η_T), and $\Delta G^{\ddagger}$, $\Delta H^{\ddagger}$, and $\Delta S^{\ddagger}$ are the activation free energy, enthalpy, and entropy, respectively.

This analysis allowed us to obtain the thermodynamic activation parameters of the thermal inactivation process reported in this work (Figure 9 and Table 2). We used a ν-value of 10^6 s^{-1}, which is a reasonable consensus value.[56,57] As expected, given the small range of preincubation temperatures used in these experiments (49−57 °C), a linear dependence on the temperature of $\Delta G^{\ddagger}$ was observed (Figure 9).

The small differences in $\Delta G^{\ddagger}$ arose from large positive differences in enthalpic and entropic contributions. Large values of $\Delta H^{\ddagger}$ are generally associated with increased energy barriers unless coupled with a large compensatory increase in the value of $\Delta S^{\ddagger}$, which is destabilizing. It is worth noting that the activation entropy was positive in all the experimental conditions tested in this work, indicating that the degrees of freedom of the protein and of the solvent are increased in the transition state respect to the native state.

The occlusion of K$^+$ and Rb$^+$ caused an increase in the energy barrier between the active and inactive states of the enzyme ($\Delta G^{\ddagger}$). This is clearly reflected in the activation energy plot (Figure 9). The increase in $\Delta G^{\ddagger}$ caused by K$^+$ and Rb$^+$ ($\Delta\Delta G^{\ddagger}$) is caused by a favorable enthalpic effect ($\Delta\Delta H^{\ddagger}$), thus suggesting the redistribution of electrostatic interactions and of the hydrogen bonding network. In contrast, the specific interaction of Na$^+$ with the enzyme caused a slight reduction in $\Delta G^{\ddagger}$. This is caused by an unfavorable entropic effect, suggesting a change in the number of particles (release of water or ions) and/or an increase in conformational entropy.

■ ASSOCIATED CONTENT

Ⓢ Supporting Information

Correlation between structural changes and Na$^+$,K$^+$-ATPase inactivation at several temperatures. Temperature dependences of apparent Na$^+$ affinity ($K_{0.5,Na}$). This material is available free of charge via the Internet at http://pubs.acs.org.

■ AUTHOR INFORMATION

Corresponding Author

*Mailing address: Rodolfo M. González-Lebrero, IQUIFIB, Facultad de Farmacia y Bioquímica, Universidad de Buenos Aires, Junín 956 (C1113AAD) Buenos Aires, Argentina. Fax: +5411 4962 5457. E-mail: lolo@qb.ffyb.uba.ar.

Notes

The authors declare no competing financial interest.

■ REFERENCES

(1) Skou, J. C.; Esmann, M. *J. Bioenerg. Biomembr.* **1992**, *24*, 249−261.
(2) Møller, J. V.; Juul, B.; le Maire, M. *Biochim. Biophys. Acta* **1996**, *1286*, 1−51.
(3) Kuhlbrandt, W. *Nat. Rev. Mol. Cell Biol.* **2004**, *5*, 282−295.
(4) Morth, J. P.; Pedersen, B. P.; Toustrup-Jensen, M. S.; Sorensen, T. L.; Petersen, J.; Andersen, J. P.; Vilsen, B.; Nissen, P. *Nature* **2007**, *450*, 1043−1049.
(5) Shinoda, T.; Ogawa, H.; Cornelius, F.; Toyoshima, C. *Nature* **2009**, *459*, 446−450.
(6) Garty, H.; Karlish, S. J. *Annu. Rev. Physiol.* **2006**, *68*, 431−459.
(7) Jorgensen, P. L.; Pedersen, P. A. *Biochim. Biophys. Acta* **2001**, *1505*, 57−74.
(8) Jorgensen, P. L.; Hakansson, K. O.; Karlish, S. J. *Annu. Rev. Physiol.* **2003**, *65*, 817−849.
(9) Glynn, I. M.; Karlish, S. J. *Annu. Rev. Biochem.* **1990**, *59*, 171−205.
(10) Esmann, M. *Biochemistry* **1994**, *33*, 8558−8565.
(11) Schneeberger, A.; Apell, H. J. *J. Membr. Biol.* **1999**, *168*, 221−228.
(12) Beauge, L. A.; Glynn, I. M. *Nature* **1979**, *280*, 510−512.
(13) González-Lebrero, R. M.; Kaufman, S. B.; Montes, M. R.; Nørby, J. G.; Garrahan, P. J.; Rossi, R. C. *J. Biol. Chem.* **2002**, *277*, 5910−5921.
(14) Forbush, B. 3rd *Prog. Clin. Biol. Res.* **1988**, *268A*, 229−248.
(15) Rossi, R. C.; Nørby, J. G. *J. Biol. Chem.* **1993**, *268*, 12579−12590.
(16) Robinson, J. D.; Pratap, P. R. *Biochim. Biophys. Acta* **1993**, *1154*, 83−104.
(17) Goldshleger, R.; Karlish, S. J. *J. Biol. Chem.* **1999**, *274*, 16213−16221.
(18) Rice, W. J.; Young, H. S.; Martin, D. W.; Sachs, J. R.; Stokes, D. L. *Biophys. J.* **2001**, *80*, 2187−2197.
(19) Apell, H. J.; Karlish, S. J. *J. Membr. Biol.* **2001**, *180*, 1−9.
(20) Kaplan, J. H. *Annu. Rev. Biochem.* **2002**, *71*, 511−535.
(21) Horisberger, J. D. *Physiology (Bethesda)* **2004**, *19*, 377−387.
(22) Haltia, T.; Freire, E. *Biochim. Biophys. Acta* **1995**, *1241*, 295−322.
(23) Hong, H.; Joh, N. H.; Bowie, J. U.; Tamm, L. K. *Methods Enzymol.* **2009**, *455*, 213−236.
(24) Cramer, W. A.; Whitmarsh, J.; Low, P. S. *Biochemistry* **1981**, *20*, 157−162.
(25) Rigell, C. W.; de Saussure, C.; Freire, E. *Biochemistry* **1985**, *24*, 5638−5646.
(26) Brouillette, C. G.; McMichens, R. B.; Stern, L. J.; Khorana, H. G. *Proteins* **1989**, *5*, 38−46.
(27) Palazzo, G.; Lopez, F.; Mallardi, A. *Biochim. Biophys. Acta* **2010**, *1804*, 137−146.
(28) Levi, V.; Rossi, J. P.; Echarte, M. M.; Castello, P. R.; Gonzalez-Flecha, F. L. *J. Membr. Biol.* **2000**, *173*, 215−225.
(29) Cattoni, D. I.; González Flecha, F. L.; Argüello, J. M. *Arch. Biochem. Biophys.* **2008**, *471*, 198−206.
(30) Jorgensen, P. L.; Andersen, J. P. *Biochemistry* **1986**, *25*, 2889−2897.
(31) Goldshleger, R.; Tal, D. M.; Karlish, S. J. *Biochemistry* **1995**, *34*, 8668−8679.
(32) Shainskaya, A.; Nesaty, V.; Karlish, S. J. *J. Biol. Chem.* **1998**, *273*, 7311−7319.
(33) Grinberg, A. V.; Gevondyan, N. M.; Grinberg, N. V.; Grinberg, V. Y. *Eur. J. Biochem.* **2001**, *268*, 5027−5036.
(34) Donnet, C.; Arystarkhova, E.; Sweadner, K. J. *J. Biol. Chem.* **2001**, *276*, 7357−7365.

(35) Fischer, T. H. *Biochem. J.* **1983**, *211*, 771−774.
(36) Fodor, E.; Fedosova, N. U.; Ferencz, C.; Marsh, D.; Pali, T.; Esmann, M. *Biochim. Biophys. Acta* **2008**, *1778*, 835−843.
(37) Jorgensen, P. L. *Biochim. Biophys. Acta* **1974**, *356*, 36−52.
(38) Klodos, I.; Esmann, M.; Post, R. L. *Kidney Int.* **2002**, *62*, 2097−2100.
(39) Schwarzbaum, P. J.; Kaufman, S. B.; Rossi, R. C.; Garrahan, P. J. *Biochim. Biophys. Acta* **1995**, *1233*, 33−40.
(40) Rossi, R. C.; Kaufman, S. B.; González Lebrero, R. M.; Nørby, J. G.; Garrahan, P. J. *Anal. Biochem.* **1999**, *270*, 276−285.
(41) Roman, E. A.; Santos, J.; González Flecha, F. L. The use of circular dichroism methods to monitor unfolding transitions in peptides, globular and membrane proteins. In *Circular Dichroism: Theory and Spectroscopy*; Rodgers, D. S., Ed.; Nova Science Publishers, Inc.: New York, 2011; pp 229−266.
(42) Levi, V.; Villamil Giraldo, A. M.; Castello, P. R.; Rossi, J. P.; Gonzalez Flecha, F. L. *Biochem. J.* **2008**, *416*, 145−152.
(43) Demchenko, A. P.; Gallay, J.; Vincent, M.; Apell, H. J. *Biophys. Chem.* **1998**, *72*, 265−283.
(44) Cattoni, D. I.; Kaufman, S. B.; González Flecha, F. L. *Biochim. Biophys. Acta* **2009**, *1794*, 1700−1708.
(45) Kaufman, S. B.; González-Lebrero, R. M.; Schwarzbaum, P. J.; Nørby, J. G.; Garrahan, P. J.; Rossi, R. C. *J. Biol. Chem.* **1999**, *274*, 20779−20790.
(46) Kaufman, S. B.; González-Lebrero, R. M.; Rossi, R. C.; Garrahan, P. J. *J. Biol. Chem.* **2006**, *281*, 15721−15726.
(47) Schack, V. R.; Morth, J. P.; Toustrup-Jensen, M. S.; Anthonisen, A. N.; Nissen, P.; Andersen, J. P.; Vilsen, B. *J. Biol. Chem.* **2008**, *283*, 27982−27990.
(48) González-Lebrero, R. M.; Kaufman, S. B.; Garrahan, P. J.; Rossi, R. C. *J. Biol. Chem.* **2002**, *277*, 5922−5928.
(49) Miles, A. J.; Wallace, B. A.; Esmann, M. *Biochim. Biophys. Acta* **2011**, *1808*, 2573−2580.
(50) Hagen, S. J. *Curr. Protein Pept. Sci.* **2010**, *11*, 385−395.
(51) Hänggi, P.; Talkner, P.; Borkovec, M. *Rev. Mod. Phys.* **1990**, *62*, 251.
(52) Kramers, H. A. *Physica* **1940**, *7*, 284−304.
(53) Ansari, A.; Jones, C. M.; Henry, E. R.; Hofrichter, J.; Eaton, W. A. *Science* **1992**, *256*, 1796−1798.
(54) Noronha, M.; Gerbelova, H.; Faria, T. Q.; Lund, D. N.; Smith, D. A.; Santos, H.; Macanita, A. L. *J. Phys. Chem. B* **2010**, *114*, 9912−9919.
(55) Gavish, B. Molecular dynamics and the transient strain model of enzyme catalysis. In *The fluctuating enzyme*; C. R., W., Ed.; Wiley: New York, 1986.
(56) Zhu, Y.; Alonso, D. O.; Maki, K.; Huang, C. Y.; Lahr, S. J.; Daggett, V.; Roder, H.; DeGrado, W. F.; Gai, F. *Proc. Natl. Acad. Sci. USA* **2003**, *100*, 15486−15491.
(57) Torrent, J.; Marchal, S.; Ribo, M.; Vilanova, M.; Georges, C.; Dupont, Y.; Lange, R. *Biophys. J.* **2008**, *94*, 4056−4065.

3429

dx.doi.org/10.1021/jp2124108 | *J. Phys. Chem. B* 2012, 116, 3421−3429